

## **2 × CO<sub>2</sub> and Solar Variability Influences on the Troposphere Through Wave-Mean Flow Interactions**

**D. RIND, P. LONERGAN, N.K. BALACHANDRAN, and D. SHINDELL**

*NASA/Goddard Institute for Space Studies at Columbia University, NY, USA*

*(Manuscript received 24 May 2001, in revised form 11 February 2002)*

### **Abstract**

A variety of climate forcings are now thought to be able to influence planetary wave dynamics in the troposphere by affecting the propagation of planetary waves out of the troposphere. However, this propagation pattern is sensitive to the details of the corresponding zonal wind changes. Here we discuss two forcing mechanisms that alter zonal winds and subsequent tropospheric responses: changes in atmospheric CO<sub>2</sub> concentrations, and solar forcing in conjunction with the QBO. Increased atmospheric CO<sub>2</sub> concentrations can be shown to influence planetary wave refraction so as to produce an intensified residual circulation in the subtropical lower stratosphere (which increases transport of tropospheric species into the stratosphere). In our GCM experiments, the low latitude response appears qualitatively robust over a wide range of tropical warming magnitudes, although the quantitative circulation change depends upon the degree of tropical warming as influenced by convection and cloud cover changes; it varies by a factor of three with a factor of three change in tropical warming. At higher latitudes, this equatorward planetary wave refraction has been associated with an increase in the high phase of the Arctic Oscillation. In the model experiments, the extratropical response depends upon the magnitude of both low and high latitude warming in the troposphere; with SST and sea ice changes that result in a weaker Hadley Cell and greater high latitude warming, the Arctic Oscillation phase change may be negative.

The QBO alters the latitudinal gradient of the zonal wind in the stratosphere, and solar heating, in association with ozone response, alters the vertical gradient of the zonal wind. Both gradients affect the refractive properties of planetary waves uniquely for each individual combination of tropical east/west winds and solar maximum/minimum activity. In the model, when we consider solar maximum compared to solar minimum conditions, the east (west) phase of the QBO results in a relative high (low) phase of the Arctic Oscillation with corresponding temperature changes. Observed and modeled surface air temperature variations calculated between the solar cycle extremes in the different QBO phases are similar in magnitude to those derived from regression of monthly data on the AO, both being on the order of observed interannual variations.

### **1. Introduction**

The impact of climate forcings on the stratosphere, and the effect this may have on the troposphere, has become a topic of increasing interest. Radiative forcing of the troposphere

by changes in stratospheric composition (e.g., ozone) has long been known to be an important consideration (e.g., Rind and Lacis 1993). What is new is the attention being paid to the potential dynamical effect the stratosphere may be having on tropospheric circulations, primarily through the influence of zonal wind changes in the stratosphere on planetary wave propagation from the troposphere. Baldwin and Dunkerton (2001) relate stratospheric circulation changes to tropospheric weather events, per-

---

Corresponding author: D. Rind, NASA/Goddard Institute for Space Studies, Columbia University, 2880 Broadway, New York, NY 10025, USA.  
E-mail: drind@giss.nasa.gov.

© 2002, Meteorological Society of Japan

haps through this mechanism. In the case of increasing CO<sub>2</sub>, Shindell et al. (1999a, 2001) illustrated the ability of a model with a full stratosphere to reproduce the observed change in equatorward planetary wave propagation, and hence the high phase (lower pressure at the pole) of the Arctic Oscillation, that has been occurring over the last few decades (Thompson et al. 2000)). The requirement in the model for inclusion of a full stratosphere (hence with a top above the middle stratosphere, Shindell et al. (1999a)) implies that planetary waves with large vertical wavelengths feel the presence of the zonal wind changes in the stratosphere, regardless of whether the meridional propagation change is actually occurring in the upper troposphere or stratosphere.

Similarly, changes in solar irradiance during a solar cycle may be having a dynamical influence on the troposphere, far exceeding the direct radiative forcing of 0.1% between solar maximum and solar minimum. Apparent changes in tropospheric circulation have been ascribed to such solar variations, either in conjunction with the QBO or independent of it, from both observations (Labitzke and van Loon 1988; van Loon and Labitzke 1998) and models (Rind and Balachandran 1995; Shindell et al. 1999b). As discussed in another paper in this volume (Kodera 2001) and in Shindell et al. (2001), volcanic aerosols and polar stratospheric ozone losses also seem to impact tropospheric circulations. The QBO by itself appears to affect tropospheric northern annular modes (Coughlin and Tung 2001). All these forcings seem to involve the same process—alteration in temperature gradients and zonal wind in the upper troposphere and stratosphere, affecting tropospheric wave propagation and tropospheric angular momentum transport.

In this paper we address issues concerning the effect of both doubled CO<sub>2</sub> and solar forcing on tropospheric circulation and temperature. For increased CO<sub>2</sub>, two circulation changes have been found in the GCM runs discussed below—an increase in the high phase of the Arctic Oscillation, as noted above, and an increase in the strength of the subtropical residual circulation in the lower stratosphere, which affects the transport of species from the troposphere into the stratosphere. Here we address how robust such circulation changes are in our

different model simulations, and on what aspects of the climate change they depend.

For solar forcing, the reality of the combined influence of the solar cycle and the QBO on tropospheric surface temperatures has been the subject of debate for more than a decade. In this paper we investigate the issue further, and compare the processes involved to those associated with the increased CO<sub>2</sub> effect on the Arctic Oscillation. To the extent that the similarity in mechanism is appreciated, the potential solar forcing effects will be less of a mystery.

## 2. Model and experiments

Most of the runs discussed in these experiments were made with the GISS Global Climate Middle Atmosphere Model (GCMAM) (Rind et al. 1988a,b). This model has been shown to be useful for simulating a number of the observed trends (e.g., Shindell et al. 2001) despite its coarse resolution ( $8^\circ \times 10^\circ$ , 23 layers between the surface and 85 km) perhaps because its background atmospheric structure and variability is fairly reasonable (Rind et al. *op cit.*), and it is the background wind profile whose alterations are important when planetary wave propagation changes are concerned.

An additional set of runs was made with a newer version of the GISS model at  $4^\circ \times 5^\circ$  resolution and 31 layers, whose results have been briefly described in Pawson et al. (2000). A more complete description of this doubled CO<sub>2</sub> run and its effect on tracer distribution is described in Rind et al. (2001).

To investigate the robustness of doubled atmospheric CO<sub>2</sub> on the tropospheric circulation, we utilize four different experiments, each with doubled atmospheric CO<sub>2</sub> but all with different sea surface temperature (SST) changes, in both magnitude and latitudinal variation. Each experiment has been reported previously, and to avoid confusion, we keep the names they were originally given in their respective papers. The first experiment, called “ $2 \times \text{CO}_2$ ” uses the sea surface temperature changes generated by the GISS Model 2 GCM (Hansen et al. 1984); its results were first published by Rind et al. (1990). The sea surface temperature changes for  $2 \times \text{CO}_2$  are shown in Fig. 1 (top); it features significant tropical warming. A second experiment, called “ALT” (for altered SSTs), also in-

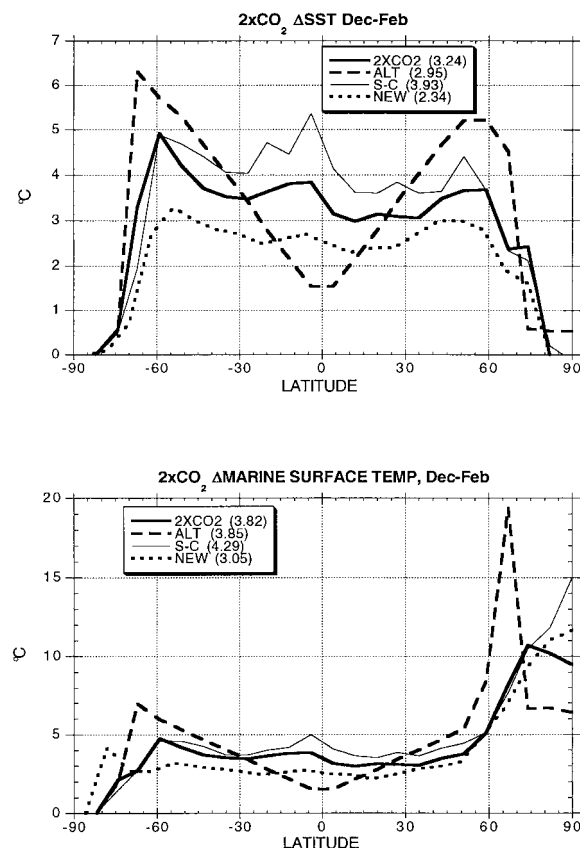


Fig. 1. Sea surface temperature (SST) anomalies (top) and marine surface temperature anomalies (including the effect of both SSTs and sea ice) during December through February in different  $2 \times \text{CO}_2$  experiments. See text for description. Global average anomalies are indicated in parenthesis.

troduced in that reference, used a sea surface temperature change closer to that which arose in the Geophysical Fluid Dynamics Laboratory doubled  $\text{CO}_2$  experiments. As shown in Fig. 1, it is characterized by less warming in the tropics, and more warming at higher latitudes. Figure 1 (bottom) indicates the change in the marine surface temperatures, including the effects of both sea surface temperature plus sea ice, a more accurate representation of the high latitude amplification of the warming associated with the boundary condition changes. The third experiment used the GCMAM with the full stratosphere to calculate the SST changes due to doubled  $\text{CO}_2$  (and is thus called “S-C” for

Table 1. Results from the different  $2 \times \text{CO}_2$  experiments in December–February.

	2xCO <sub>2</sub>	ALT	S-C	NEW	Std. Dev.
ΔGLOBAL SURF AIR TEMP (°C)	4.4	4.3	5.2	3.5	0.12
ΔSURF AIR TEMP AT EQUATOR (°C)	3.9	1.7	5.5	2.5	0.15
Δ270MB TEMP AT EQUATOR (°C)	8.0	4.4	11.3	3.0	0.3
ΔRESIDUAL CIRCULATION, 0–40°N, 46 MB	11%	7%	24%	13%	2.3%
ΔVERT. INT. TEMP CHANGE (°C) 35°N MINUS 74°N	0.76	-1.4	1.65	-0.7	0.6
ΔRESIDUAL CIRCULATION, 64°N, 192MB	-17.5%	5%	-12.5%	20%	9.6%
ΔSEA LEVEL PRESSURE (mb) (60–80N MINUS 30–50N)	-3.7	-2.8	-5.5	1.3	1.8
ΔVERT. INT. TEMP. CHANGE (°C) 0° MINUS 82°N	2.1	-1.6	2.1	-1.2	1.3
ΔEKE, TROP, WAVE #1–4	7.9%	0.2%	5.3%	-1.3%	5.3%

stratosphere/calculation). As discussed in Rind et al. (1998) it has greater tropical SSTs and global warming than any of the other experiments. The final doubled  $\text{CO}_2$  run is done with the new model (hence called “NEW”); its warming, both in the tropics and globally, is more modest (see Rind et al. 2001). The relevant model  $2 \times \text{CO}_2$  characteristics and dynamical changes discussed in this paper for these experiments are given in Table 1.

The experiments were each run for 10 years after reaching equilibrium, which occurs in a few years in the case of specified SSTs, and after 25 years with calculated SSTs (as in S-C). Results are presented for the 10 years following equilibrium, and are compared with the last 10 years of a control run of equal length.

To investigate the effect of solar/QBO forcing on tropospheric circulation and temperatures, we make use of the experiments described in Rind and Balachandran (1995). To mimic the effect of both solar and ozone changes on stra-

tospheric radiation absorption, the experiments increased/decreased solar UV (short of 0.3 microns) by 5%. (The experiments with realistic solar forcing and calculated ozone changes, described in Shindell et al. (1999b), had slightly weaker heating rate changes corresponding to an equivalent solar forcing of about 4%; the patterns of response were similar.) We use this version because an extensive comparison has been made of its results compared with observations when the QBO is used (Balachandran et al. 1999). The QBO was forced in the model as described in Balachandran and Rind (1995) by relaxing back to specified east/west wind perturbations as a function of latitude within the QBO altitude range. The significance of all results is ascertained by comparison to the model's variability in the unforced control run(s).

### 3. Results

#### 3.1 $2 \times \text{CO}_2$

In this section we describe the results for the two major circulation feature changes of interest due to greenhouse gas forcing—the residual circulation in the tropical lower stratosphere, and the phase of the Arctic Oscillation at high latitudes. We concentrate on the Northern Hemisphere during winter (December–February). Results are summarized in Table 1, which gives the global and equatorial surface air temperature changes, as well as the temperature change in the tropical upper troposphere (270 mb); the low latitude residual circulation change in the middle stratosphere, and the high latitude residual circulation change in the lower stratosphere; the change in vertically-integrated air temperature between mid and high latitudes, and between low and high latitudes; the change in sea level pressure between high latitudes and mid-latitudes, related to the phase of the Arctic Oscillation; and the tropospheric eddy kinetic energy averaged over wavenumbers 1–4.

##### *a. Lower stratosphere subtropical residual circulation*

As shown in Table 1, the residual circulation in the low-to-mid stratosphere averaged from the equator to 40°N increases in all four  $2 \times \text{CO}_2$  experiments. Compared to interannual standard deviations for the control run, the

changes in each experiment are highly significant. The magnitude of the increase is partly associated with the magnitude of the tropical warming. For the experiments with the older model ( $2 \times \text{CO}_2$ , ALT and S-C), the greater the sea surface temperature increase, and the corresponding greater warming in the tropical upper troposphere, the greater percentage change in residual circulation, as explained below. The newer model also shows an increase, but it is proportionately more than expected given the magnitude of the surface warming. Hence inter-model variability plays a role in the magnitude of the change, perhaps associated with the climatological background state—the newer model has a weaker residual circulation at this altitude, and stronger planetary wave energy, both of which help contribute to a greater proportional residual circulation response.

In all these experiments, the tropical upper tropospheric warming, at say 150 mb, is in contrast to the cooling or reduced warming at higher latitudes where this pressure level is above the tropopause during Northern Hemisphere winter. The increased temperature gradient provides, via the thermal wind relationship, increased west winds in the upper troposphere/lower stratosphere, with relative equatorward planetary wave refraction (Fig. 2). EP flux convergences then drive the stronger subtropical residual circulation. With stronger upper tropospheric warming, the west wind increase is greater (e.g., Fig. 2 for  $2 \times \text{CO}_2$  and S-C), and, in general, so are the EP flux convergences and residual circulation change. This result is similar to that obtained by Butchart and Sciafe (2001) using the Hadley Center model.

##### *b. Phase of the Arctic Oscillation*

In the extratropics, the  $2 \times \text{CO}_2$  experiments show different circulation changes, depending upon the magnitude of warming at mid latitudes compared with high latitudes in the troposphere (as indicated by the change in vertically-integrated temperature gradient between 35° and 74°N in Table 1). The runs with greater mid-latitude warming ( $2 \times \text{CO}_2$  and S-C) have a west wind increase in the lower stratosphere that extends to higher latitudes (Fig. 2), and so the equatorward wave

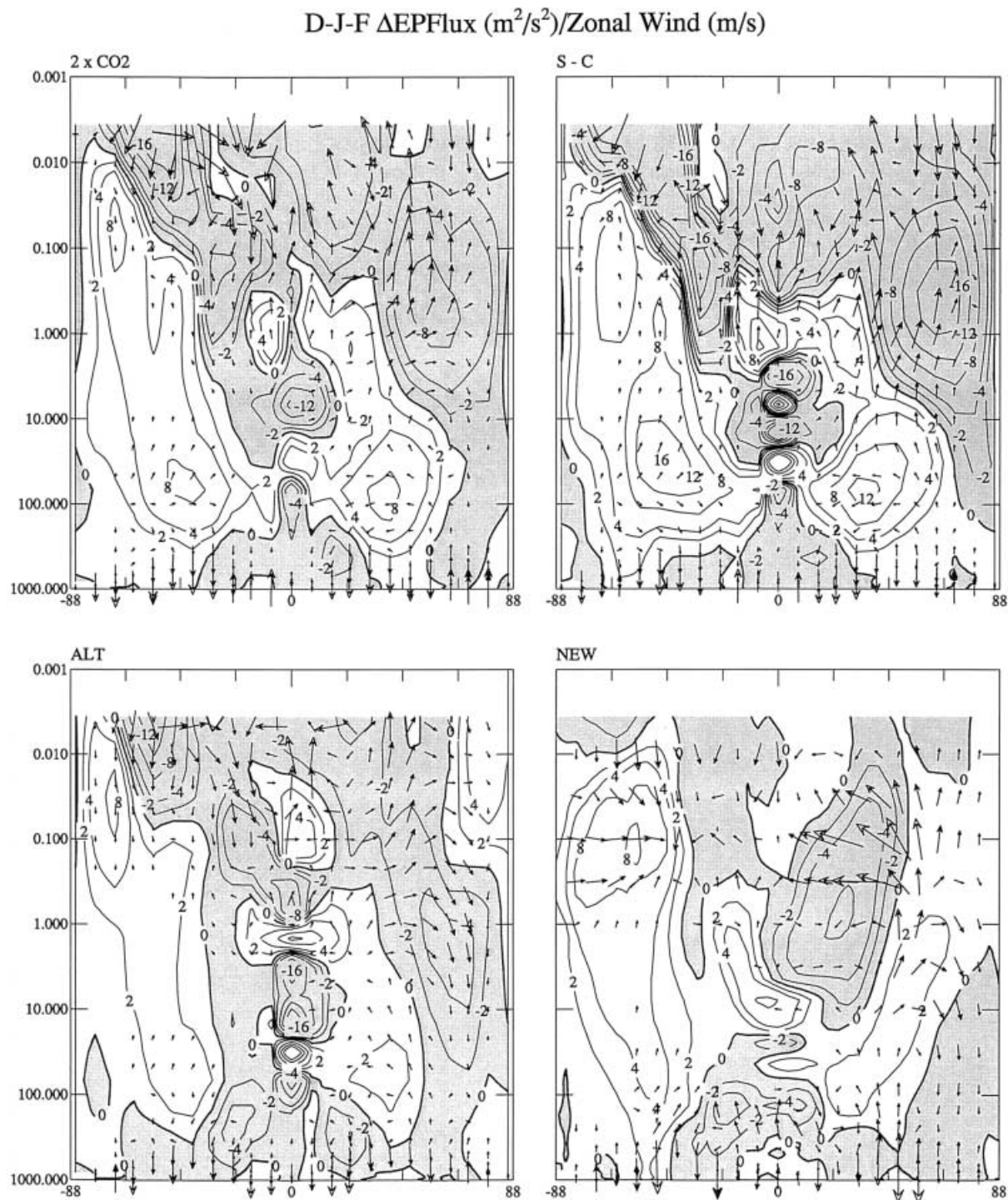


Fig. 2. Change in EP flux (arrows) and zonal wind (contours, with negative values shaded) in the different  $2 \times \text{CO}_2$  experiments. For the EP flux vectors, values less than  $5 \times 10^{-3} \text{ m}^2\text{s}^{-2}$  are not shown. Arrows of maximum length correspond to flux changes of approximately  $9 \text{ m}^2\text{s}^{-2}$ ; minimum values shown are scaled for presentation purposes to be ten times smaller. For consistency with the resolution of the other simulations, arrows for only half of the latitudes are shown in NEW (bottom right).

Table 2. Change during Dec–Feb in the different experiments of the temperature ( $^{\circ}\text{C}$ ) at  $35^{\circ}\text{N}$ / at  $74^{\circ}\text{N}$ / and the gradient between  $74$  and  $35^{\circ}\text{N}$  for different pressure levels.

	$\Delta T\ 35^{\circ}\text{N}/\Delta T\ 74^{\circ}\text{N}/\Delta T\text{Grad}\ 74^{\circ}\text{N}\ \text{MINUS}\ 35^{\circ}\text{N}$			
PRES	$2\text{CO}_2$	ALT	S-C	NEW
1000	3.4/ 10.3/ 6.9	4.2/ 7.0/ 3.2	4.6/ 10.3/ 5.7	3.3/ 8.6/ 5.0
750	3.9/ 5.8/ 2.1	4.2/ 6.3/ 2.1	5.0/ 6.2/ 1.2	3.3/ 6.3/ 3.0
500	5.0/ 4.3/ -0.7	5.2/ 4.2/ 1.0	6.3/ 5.7/ -0.6	3.1/ 3.1/ 0
250	5.1/ 0.7/ -4.4	3.2/ 3.1/ 0.1	6.9/ 3.1/ -3.8	2.5/ 1.5/ -1.0
150	3.8/ -2.4/ -6.2	1.9/ 1.6/ 0.3	5.2/ -1.2/ -6.4	1.5/ 0/ -1.5

refraction occurs at those latitudes as well. The high latitude EP flux divergence that results helps generate a reduced high latitude residual circulation (Table 1).

In contrast, NEW has greater warming at high latitudes, with a change to more east winds, and wave refraction is preferentially towards the pole. The resultant EP flux convergence helps generate an increased high latitude residual circulation. In ALT, there is little change in the extratropical upper tropospheric latitudinal gradient, a weaker and more latitudinally-restricted west wind increase (Fig. 2), and a slight increase in residual circulation.

Why is the extratropical temperature gradient so different among these runs? As indicative of the variation across mid-latitudes, in Table 2 we compare the modeled temperature changes at  $35^{\circ}\text{N}$ , at  $74^{\circ}\text{N}$ , and the temperature gradient change ( $74^{\circ}\text{N}$  minus  $35^{\circ}\text{N}$ ) during December through February for selected pressure levels. At the lowest levels, the temperature response is strongly constrained by the marine surface temperature changes (Fig. 1, bottom), and all the runs show the expected high latitude amplification of the warming with a reduced latitudinal gradient. Hence all the runs have weaker west winds in the lower-most troposphere at these latitudes. In  $2\text{CO}_2$  and S-C the gradient change reverses by 500 mb, and henceforth midlatitudes warm more, resulting in an increase in the west wind shear with altitude. This arises not so much because the high latitude warming is any less—it is greatest in S-C of any of the runs—but because of added mid-latitude warming in the middle and upper troposphere. This warming is the result

of an intensified Hadley Cell in  $2 \times \text{CO}_2$  and S-C on the order of 10–15%, which produces a large increase in poleward heat transport and energy convergence at mid latitudes in the upper troposphere in those two experiments. In contrast, ALT has a Hadley Cell decrease of some 20%, and hence its warming decreases with altitude above 500 mb; it therefore maintains a decreased gradient throughout the troposphere with weakened west winds between these latitudes at all altitudes. NEW shows little change in Hadley Cell intensity, and its warming decreases slowly with height at  $35^{\circ}\text{N}$ .

The Hadley Cell responses are attributable to the change in the latitudinal gradient of input SSTs between  $10^{\circ}\text{S}$  and  $20^{\circ}\text{N}$  in these experiments during December–February. The SST gradient in this region increases in S-C by  $1.7^{\circ}\text{C}$ , in  $2 \times \text{CO}_2$  by  $0.7^{\circ}\text{C}$ , in New by just  $0.25^{\circ}\text{C}$ , and it decreases in ALT by  $1.25^{\circ}\text{C}$ . The SST gradient change alters the meridional circulation cell and relative vertical air motions which then affect precipitation and latent heat release, further amplifying the circulation change (c.f., Rind and Rossow 1984; and Rind 1998 for a full discussion of this effect).

To complete this assessment, it is necessary to explain why the tropical warming varies so much in these experiments. In  $2 \times \text{CO}_2$ , cirrus cloud cover increases in the tropics augmented the tropical surface warming in the GCM that was providing the SSTs for that experiment, but clouds in that model were limited to 200 mb altitude—hence so were any increased clouds. In S-C, calculated with the GCMAM which had greater vertical resolution, clouds could occur at any level, and increased at higher altitudes with doubled  $\text{CO}_2$ , augmenting the tropical warming further. In both cases, cirrus clouds had optical thicknesses of 0.33, and hence acted primarily as thermal radiation absorbers rather than solar energy reflectors. In contrast, in NEW, two types of cirrus clouds were allowed: cirrus associated with tropical anvils, with optical thickness greater than 4 (which preferentially cool the climate by reflecting solar radiation); and thinner cirrus. Both increased in the doubled  $\text{CO}_2$  simulation, and so effectively canceled out any cirrus cloud feedback. Therefore NEW had smaller tropical warming, and the response was also more uniform with latitude, reducing any SST gradi-

ent change (NEW also included a cloud optical thickness feedback, further altering the results). Finally, ALT had less tropical warming by specification from the GFDL model results; it is hypothesized that the moist adiabatic adjustment scheme used for convection in that model limits upper level moisture and cloud cover change, reducing tropical warming in comparison to that which occurs with the penetrative convection in the GISS model. In summary, then, cloud and convection scheme differences appear responsible for the different tropical response in the models, and ultimately the differing effect on wave energy propagation, residual circulation change, and even high latitude pressure response.

For the runs without strong mid-latitude warming above 500 mb, ALT had the largest overall west wind reduction, while NEW had the largest increase in high latitude residual stream function. Apparently the much stronger high latitude amplification at low levels in NEW, and its stronger easterly wind shear in the lower troposphere, altered planetary wave refraction more severely than in ALT. This in turn was related to the amount of warming in the surface marine temperatures (Fig. 1, bottom). The absolute sea ice reduction from 80–90°N during December–February was about 3% in all of the experiments except ALT, where no reduction was specified (to keep the global warming similar to the in  $2 \times \text{CO}_2$ ). This had the effect of limiting the high latitude temperature response in the lower troposphere, and reducing the ability of ALT to generate a stronger negative phase of the Arctic Oscillation. Sea ice changes are thus another component of the model that will influence its high latitude circulation response via altered planetary wave propagation. (Note that reducing sea ice also increases heat flux from the ocean, decreasing the atmospheric stability, and therefore directly leading to increased cyclonicity and lower pressure at high latitudes).

The initial anomaly in the different experiments led to a reinforcement of the pattern due to the EP flux changes themselves. The EP flux divergence in  $2 \times \text{CO}_2$  and S-C at high latitudes provided for greater west winds and relative cooling, while the opposite occurs in NEW and ALT (compare, for example, the change in warming between 500 mb and 150 mb in the

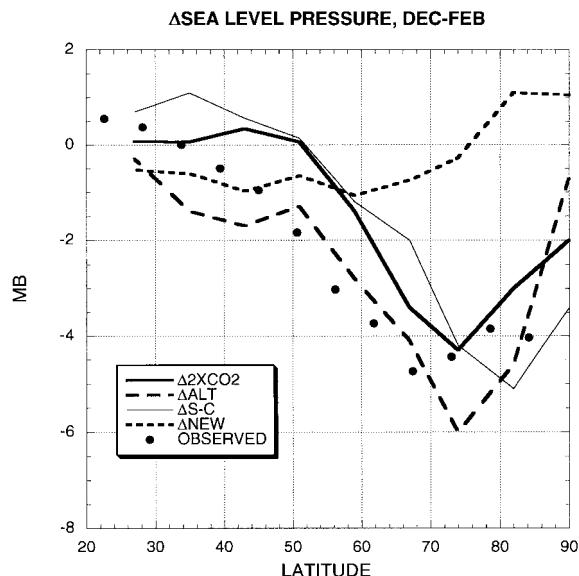


Fig. 3. Sea level pressure changes during December through February in the Northern hemisphere for the different  $2 \times \text{CO}_2$  experiments. Also shown are the linear trends during Northern hemisphere winter over the past 46 years (after Trenberth and Paolino, 1980, updated through 1997). The observed trend is indicative of the recent tendency for the positive phase of the AO.

different runs at 74°N in Table 2). This positive feedback reinforces the latitudinal gradient differences and helps the model results diverge.

With the different high latitude residual circulation responses, we might expect different impacts on the sea level pressure conditions that determine the phase of the Arctic Oscillation. Shown in Fig. 3 are the sea level pressure changes from the control run as a function of latitude during December through February in the Northern Hemisphere. Changes at the individual latitudes are on the order of 2 standard deviations of the model's unforced variability, as are the differences between high and mid-latitudes. With more equatorward planetary wave refraction from high latitudes in  $2 \times \text{CO}_2$  and S-C, the sea level pressure is reduced poleward of 50°N, and increases somewhat to the south (representative of the positive phase of the Arctic Oscillation). In ALT, the difference between the polar and mid-latitude response is smaller, while in NEW the effect is

reversed (negative phase of the Arctic Oscillation); the difference between NEW and the other experiments is significant at the 95% level. The regional surface air temperature changes associated with these specific sea level pressure and advection patterns are quite different in the various simulations, although the radiative warming and feedbacks are largely similar.

The discussion so far has focused on changes in the refraction pattern of planetary waves due to the altered climate, but the generation of waves in the troposphere also differs somewhat in the different experiments. As indicated in Table 1, the runs with greater tropical warming also have increased planetary longwave energy in the troposphere; with the difference between NEW and the experiments with the largest tropical warming marginally significant (90% level). The greater tropical warming produces increased zonal available potential energy, which ultimately results in increased baroclinic energy conversion for the longest waves (Rind et al. 1998; see also Wiin-Nielsen 2001 for the importance of instability for waves with low wave numbers). The altered wave energy will also affect the EP flux convergences and residual circulation changes in the stratosphere.

Observational analysis shows that the current positive phase of the Arctic Oscillation is occurring with tropical tropospheric cooling, an increase in the tropospheric residual circulation, and a reduction in the subtropical lower stratospheric residual circulation (Thompson et al. 2000; also see Wallace 2001 in this volume). These observations are not in conflict with our model results, despite the fact that some of our runs indicate both an increase in the high phase of the Arctic Oscillation and an increase in the subtropical residual circulation in the lower stratosphere. The observed AO relationship with tropical tropospheric cooling is a dynamical effect (rising air) associated with the circulation induced by wave propagation effects that lead to the positive phase of the Arctic Oscillation. In the doubled CO<sub>2</sub> climate, greenhouse warming of the tropics is occurring, overwhelming such dynamical influences. In that sense, model and observations are consistent: with increased (decreased) tropical temperatures due to radiative (dynamical) effects, the subtropical lower stratospheric residual circulation increases (decreases).

We conclude from these experiments that, at least in the GISS models, the intensification of the subtropical residual circulation in the lower stratosphere in  $2 \times \text{CO}_2$  experiments is robust. The tropical upper troposphere always warms in comparison with higher latitudes at the same pressure which are in the stratosphere, and hence cooling or have reduced warming—this result occurs in GCMs from all groups. It leads to relative equatorward planetary wave refraction and convergence, intensifying the circulation. The subtropical residual circulation in the lower stratosphere also increased in the transient global warming experiment reported by Butchart and Sciafe (2001) using the Hadley Centre model. The magnitude of the effect is associated with the degree of tropical warming, although varying background climatologies (and model physics) also have an impact. In contrast, the high latitude residual circulation change is not robust in the GISS models, being influenced by the sea surface temperature and sea ice changes that affect mid latitude and polar warming. IPCC (2001) also noted the lack of consistent AO response in future climate simulations, among different models.

## 2. Solar cycle/QBO

In this section we describe the results from runs with solar maximum and solar minimum conditions in conjunction with east or west phases of the QBO. The model's results were originally discussed by Balachandran and Rind (1995), Rind and Balachandran (1995), Shindell et al. (1999b; without the QBO influence) and Balachandran et al. (1999). In this presentation we look at those runs in the context of the wave-mean flow interactions discussed above for the greenhouse gas experiments, including the potential effects on the Arctic Oscillation.

Shown in Fig. 4 (left) are the EP flux changes between solar maximum and solar minimum conditions with no QBO forcing (top) and during the east and west phases of the QBO in the model. In the lower stratosphere, relative equatorward wave energy propagation occurs throughout the extratropics between solar maximum and solar minimum conditions during the east phase of the QBO (and without any QBO forcing, as the model naturally has light easterlies present at those levels) and relative poleward propagation during the west phase.



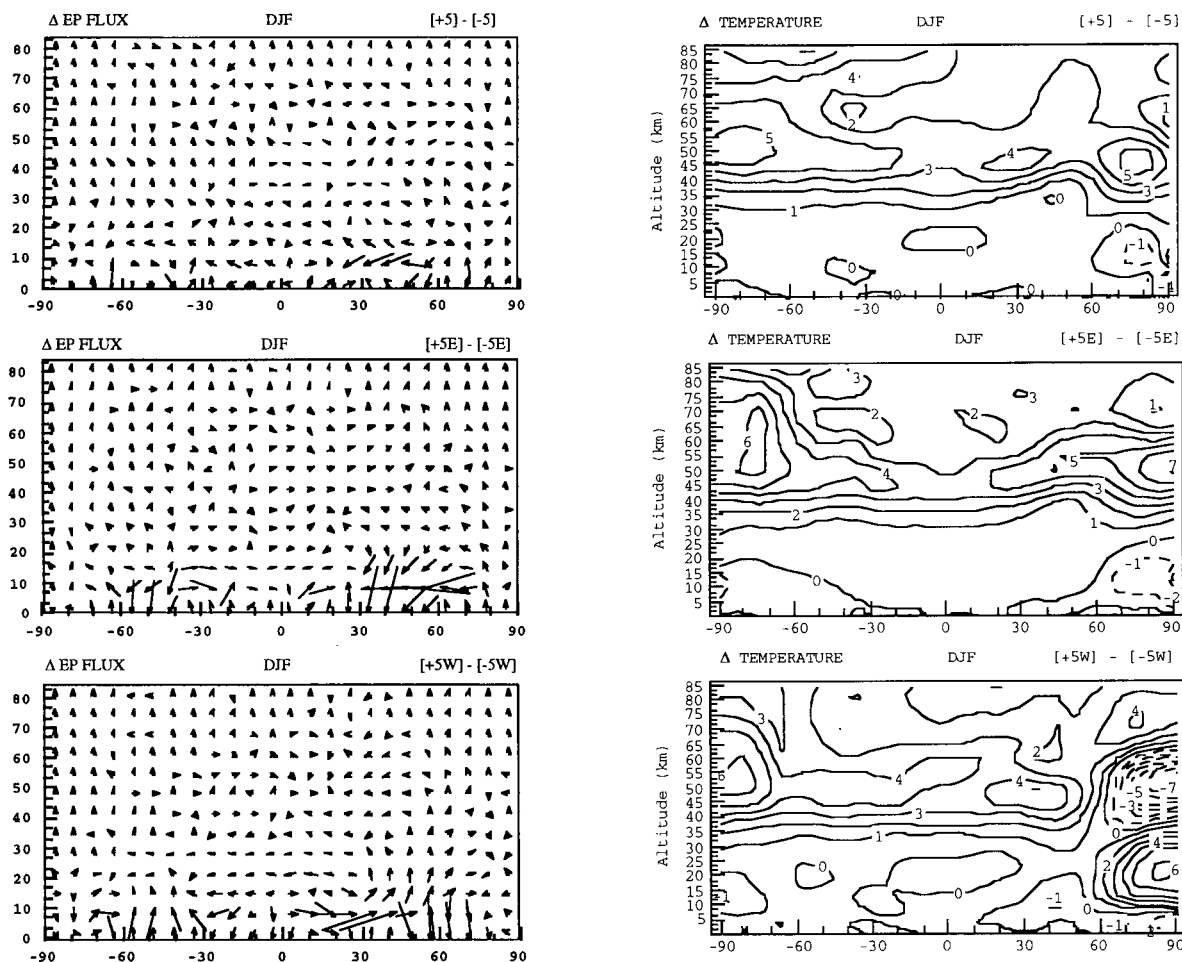


Fig. 4. Modeled EP flux changes between solar maximum and solar minimum conditions with no QBO, and during the east and west phases of the QBO in the model (left); also shown are the corresponding temperature changes (right). After Balachandran and Rind (1995).

During solar maximum conditions greater radiative (ozone) heating occurs in the mid-to-upper stratosphere at low latitudes relative to high winter latitudes (where there is no sunshine). This increases the latitudinal temperature gradient, and from the thermal wind relationship, increases the vertical shear of the zonal wind. Thus as discussed in Balachandran and Rind (1995) and Rind and Balachandran (1995), while the QBO alters the latitudinal gradient of the zonal wind, the solar cycle affects the vertical gradient, and both impact the refraction properties of planetary waves. Each unique combination of QBO east/west phase and solar max/min conditions therefore is associated with a unique propagation pattern. For

example, while equatorward propagation in the lower stratosphere is favored during the west QBO phase compared to the east phase, during solar maximum the west winds increase with altitude in the polar region, so the wave refraction pattern is equatorward and then upward and poleward; during solar minimum it is equatorward and relatively downward. The difference, as shown in Fig. 4 (left bottom), provides for a vertical and meridional propagation change that results in different patterns of EP flux convergences.

The impact of this wave propagation change on the zonal temperature structure is shown in Fig. 4 (right). For solar maximum minus solar minimum during the east phase (and

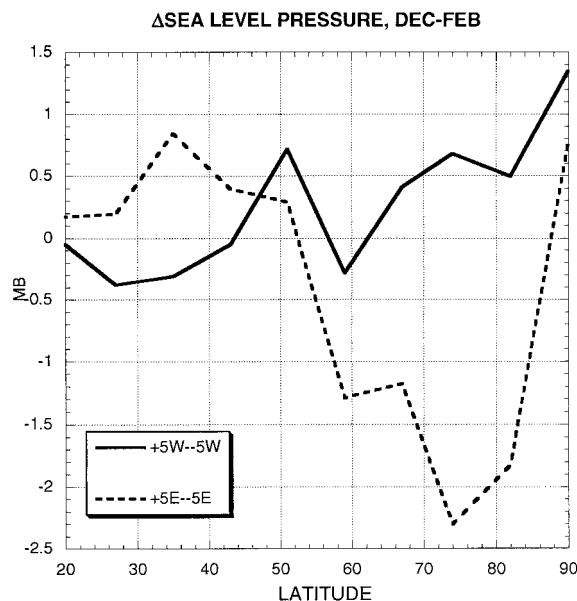


Fig. 5. Sea level pressure changes between solar maximum and solar minimum conditions during the east and west phases of the QBO in the model.

also without any QBO forcing), with relative EP flux divergence from high latitudes in the lower stratosphere, temperatures are cooler between the surface and 20 km (and geopotential heights are lower). During the west phase, with relative EP flux convergence at high latitudes, the corresponding temperatures are warmer (and geopotential heights are greater). The sea level pressure changes, indicative of the phase of EOF #1, is shown in Fig. 5 for the two cases; changes at the individual latitudes are on the order of one standard deviation of the model's unforced variability, as are the differences between high and mid-latitudes. For solar maximum minus solar minimum conditions during the east QBO, the positive phase of the Arctic Oscillation is favored, while during the west QBO, the relative negative phase occurs. Bochnicek and Hejda (2002) analyzed Northern Hemisphere observations and found that during the east phase of the QBO, solar maximum minus solar minimum conditions did favor the positive phase of the NAO (or, as can be deduced from their results, the positive phase of the AO), in agreement with these simulations, while during the west QBO phase, little NAO phase bias was seen. Labitzke and van Loon

(1988) showed sea level pressure changes for solar maximum minus solar minimum conditions and the QBO west phase (their Fig. 5e); the results are indicative of the negative phase of the Arctic Oscillation, in agreement with these model results.

van Loon and Labitzke (1988) previously correlated surface air temperatures during winter with the solar cycle during the different QBO phases. We show in Fig. 6 the observed surface air temperature changes derived from 6 different years of January/February combinations associated with the solar maximum and minimum peaks in the appropriate QBO phase. During the east phase, solar maximum minus solar minimum conditions exhibit extensive warming over Asia and cooling over northeastern North America and the northwest Atlantic that looks broadly similar to the surface air temperature changes associated with the positive phase of the Arctic Oscillation (Thompson and Wallace 2000). During the west QBO phase the patterns are noticeably different. Comparison with the surface air temperature changes shown for these months in Rind and Balachandran (1995) indicates the model has some success in reproducing the east phase results, as it has in simulating the observed temperature changes during the recent high phase of the Arctic Oscillation (Shindell et al. 1999a). There is less model success in simulating the temperature change in the west phase, for which the pressure anomalies in the model (Fig. 5) and observations are weaker.

The differences noted in the observations shown above are of similar magnitude to those associated with the phase of the Arctic Oscillation in observations (Thompson and Wallace 2000) (peak values 2–3°C in both). This is of the order of the observed interannual variation, which may be thought of as including effects such as these. van Loon and Labitzke (1988) showed that correlations of surface air temperature with solar forcing during the separate QBO phases resulted in coherent patterns explaining up to 50% of the interannual variance in specific regions. The significance of the solar/QBO effect is obviously constrained by the limited number of years of QBO data available (beginning in the 1950s) in conjunction with the number of years of peak solar maximum and minimum conditions. What we have attempted

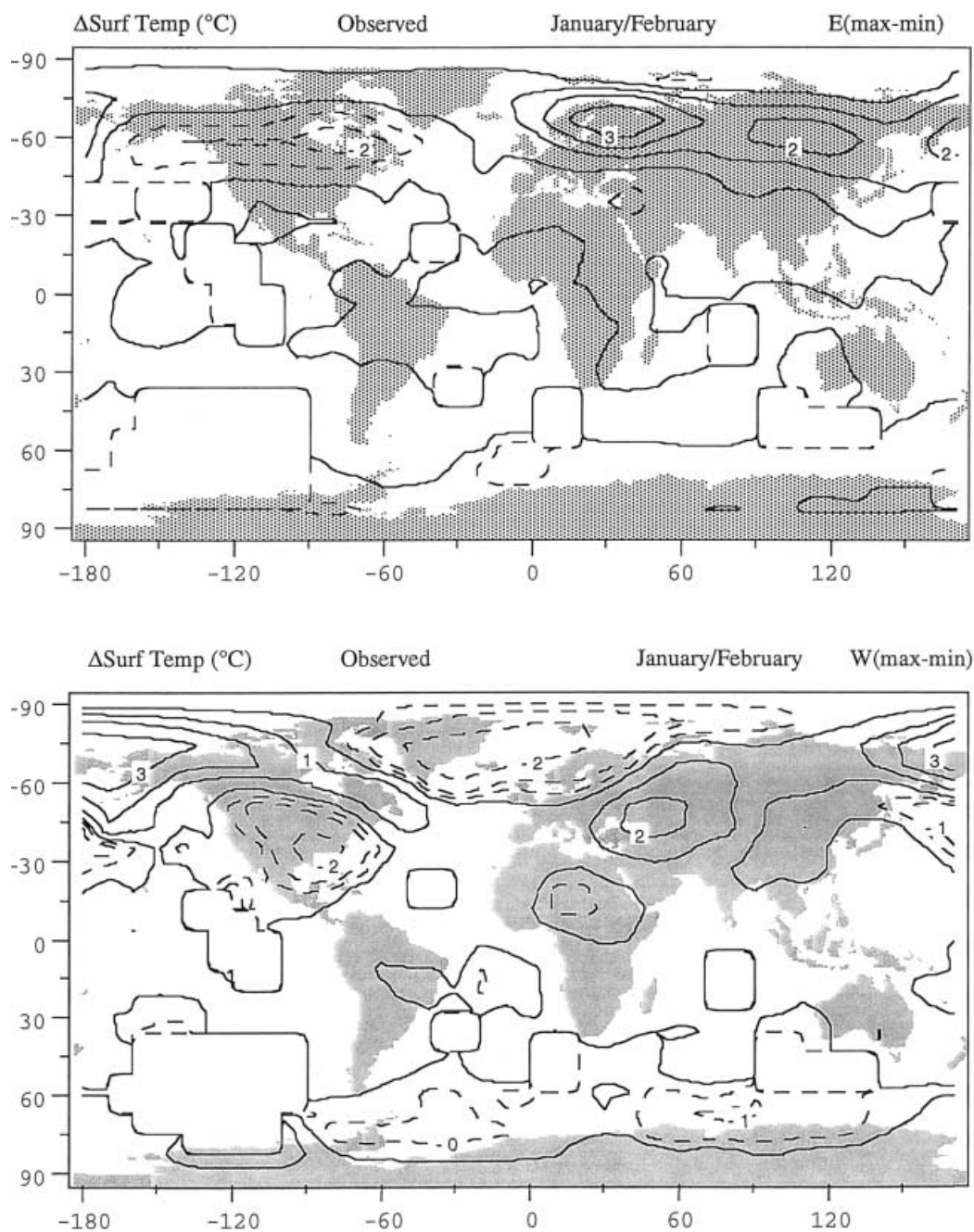


Fig. 6. Observed surface air temperature changes between solar maximum and solar minimum conditions during the east (top) and west (bottom) phase of the QBO in January and February. Results are from 5 to 6 years of each QBO phase during solar maximum and solar minimum conditions. Temperature data courtesy of M. Sato and J. Hansen.

to show is that the planetary wave propagation patterns associated with the solar cycle/QBO are such as to produce variations in the phase of the Arctic Oscillation that are broadly con-

sistent with the temperature changes derived from these limited observations. To that extent, the resulting patterns may be better understood within the broader framework of the im-

pect of altered stratospheric zonal wind patterns on wave propagation and temperature in the troposphere.

#### 4. Discussion and conclusions

Both increased CO<sub>2</sub> and solar forcing affect the modeled troposphere via an impact on the zonal wind structure of the atmosphere and planetary wave refraction patterns. In the doubled CO<sub>2</sub> climate, varying the magnitude and latitudinal gradient of warming at low latitudes impacts the magnitude of the residual circulation change, but in all cases leads to an amplification of the residual circulation in the lower stratosphere. This effect arises because warming in the upper troposphere circa 150 mb contrasts with cooling or reduced warming at the same pressure level at high latitudes where it is in the lower stratosphere. The increased temperature gradient results in stronger west winds, more equatorward planetary wave refraction, greater subtropical EP flux convergences, and hence the residual circulation increase. With greater tropical warming, the effects in general are larger, although differences in model background wind profiles (and wave generation) also have an effect. An increased residual circulation in the lower stratosphere should reduce the residence time of tropospheric trace gases (Holton et al. 1995), and does so in the GISS model (Rind et al. 2001).

Shindell et al. (2001) show that the zonal wind and EP flux refraction changes indicated here for increased CO<sub>2</sub> appear to have been occurring over the last several decades in the real world. Would this happen regardless of the cause of climatic warming, e.g., from El Ninos or solar forcing producing a similar increase in tropical SSTs, rather than increased CO<sub>2</sub>? Since the key to this effect is the increase in the tropospheric temperature gradient, the question becomes how much does that increase depend on the tropical upper tropospheric warming, which could result from any forcing of tropical sea surface temperature increase, and how much is associated with the extratropical stratospheric cooling as arises with increased CO<sub>2</sub> (or perhaps ozone depletion in certain seasons)? We investigated this issue by increasing the sea surface temperatures without doubling atmospheric CO<sub>2</sub> in the 2 × CO<sub>2</sub> and ALT experiments. The upper troposphere/lower

stratosphere zonal wind change was only 1/2 as strong in both experiments, while the resulting EP flux pattern was very similar. The sea level pressure changes are less positive at middle latitudes in 2 × CO<sub>2</sub>, and less negative at high latitudes in ALT, although in both cases the latitudinal tendencies are maintained. Therefore the distinguishing feature of the increased CO<sub>2</sub> forcing is the magnitude of the effect, not the pattern of change.

The doubled CO<sub>2</sub> climate also affects the residual circulation at high latitudes in winter, and thus the phase of the Arctic Oscillation, but in the different model runs the effects are not consistent. Recent trends at high latitudes are consistent with the simulations that produce a more positive phase of the Arctic Oscillation (Shindell et al. 1999a) as we show in Fig. 3, and feature greater warming at mid-latitudes than at the pole in the upper troposphere, with a west wind increase and relative equatorward wave propagation throughout the extratropics. In contrast, the simulations with greater climatic warming at high latitudes (than mid-latitudes) result in weaker zonal winds, relative poleward wave propagation with EP flux convergences, an extratropical stratospheric residual circulation increase, and a more negative phase of the Arctic Oscillation. Recent trends notwithstanding, what can be expected for a full doubled CO<sub>2</sub> climate change is not yet obvious, since with additional warming, greater sea ice changes may result in amplifying the high latitude temperature response.

For both the low and high latitude responses, we have emphasized the importance of the sea surface/sea ice change, which results from the added greenhouse gas forcing in conjunction with the model sensitivity. While the first three experiments (in Table 1) were all performed with the same GISS model, NEW used a later version with finer resolution and different physics. Some portion of its altered response may have arisen from the way sea surface temperature anomalies are translated into the atmospheric response, for example, how high into the atmosphere the warming occurs, and what the Hadley Cell response is, both of which can be a function of boundary layer and convection schemes. The marine surface boundary condition anomalies from S-C and NEW have been provided to the "GCM Reality In-

tercomparison Project (GRIPS; Pawson et al. 2000) for use by other modeling groups. That should provide an opportunity for the degree of inter-model variability to be assessed relative to the variability in response due to the different marine surface conditions.

Solar forcing, in combination with the QBO, produces similar effects to greenhouse gas forcing in the model in the sense that it alters planetary wave propagation patterns and affects tropospheric pressures and temperatures. In particular, during the east phase of the QBO, solar maximum minus solar minimum conditions result in relative EP flux divergences at high latitudes, and a positive phase of the Arctic Oscillation. Observed and modeled surface air temperatures changes are generally consistent with this pattern, as they are consistent with the observed temperature changes accompanying the positive phase of the Arctic Oscillation for the least few decades. The negative phase of the Arctic Oscillation, with different advection changes and a different surface air temperature response accompanies solar maximum minus solar minimum conditions in the model during the west QBO phase, when EP flux convergences occur in polar regions. To the extent that the solar/QBO effects are understood in terms of planetary wave propagation and basic quasi-geostrophic refraction tendencies, they may prove useful for interannual forecasting, as has previously been suggested (van Loon and Labitzke 1988).

### Acknowledgments

We thank Jean Lerner for graphics help. This work was supported by the NASA ACMAP and LWS programs.

### References

- Balachandran, N.K. and D. Rind, 1995: Modeling the effects of solar variability and the QBO in the Troposphere/Stratosphere system. Part 1: The Middle Atmosphere. *J. Climate*, **8**, 2058–2079.
- , D. Rind, P. Lonergan, and D.T. Shindell, 1999: Effects of solar cycle variability on the lower stratosphere and the troposphere. *J. Geophys. Res.*, **104**, 27321–27340.
- Baldwin, M.P. and T.J. Dunkerton, 2001: Stratospheric harbingers of anomalous weather regimes. *Science*, **294**, 581–584.
- Bochnicek, J. and P. Hejda, 2002: Association between extraterrestrial phenomena and weather changes in the Northern Hemisphere in winter. *Surveys in Geophysics*, in press.
- Butchart, N. and A.A. Sciafe, 2001: Removal of chlorofluorocarbons by increased mass exchange between the stratosphere and troposphere. *Nature*, **410**, 799–802.
- Coughlin, K. and K.-K. Tung, 2001: QBO signal found at the extratropical surface through northern annual modes. *Geophys. Res. Lett.*, **28**, 4563–4566.
- Hansen, J., A. Lacis, D. Rind, G. Russell, P. Stone, I. Fung, R. Ruedy, and J. Lerner, 1984: Climate sensitivity: analysis of feedback mechanisms”, in *Climate Processes and Climate Sensitivity* (eds. J. Hansen and T. Takahashi) Geophysical Monograph 29, AGU, 130–163.
- Holton, J.R., P.H. Haynes, M.E. McIntyre, A.R. Douglass, R. Rood, and L. Pfister, 1995: Stratosphere-troposphere exchange. *Rev. Geophys.*, **33**, 403–439.
- IPCC, 2001: *Climate Change 2001: The Scientific Basis*. Chapter 9. Projections of Future Climate Change, U. Cubasch and G.A. Meehl, Co-ordinating Lead Authors. Section 9.3.5.3, Decadal and longer time-scale variability. 568–570.
- Labitzke, K. and H. van Loon, 1988: Association between the 11-year solar cycle, the QBO, and the atmosphere. Part I: The troposphere and stratosphere in winter. *J. Atmos. Terr. Phys.*, **50**, 197–206.
- Pawson, S. et al., 2000: The GCM-Reality Intercomparison Project for SPARC (GRIPS): Scientific Issues and Initial Results. *Bull. Amer. Meteor. Soc.*, **81**, 781–796.
- Rind, D., 1998: Latitudinal temperature gradient and climate change. *J. Geophys. Res.*, **103**, 5943–5971.
- and W. Rossow, 1984: The effects of physical processes on the Hadley circulation. *J. Atmos. Sci.*, **41**, 479–507.
- , R. Suozzo, N.K. Balachandran, A. Lacis, and G.L. Russell, 1988: The GISS Global Climate/Middle Atmosphere Model Part I: Model structure and climatology. *J. Atmos. Sci.*, **45**, 329–370.
- and ———, 1988: The GISS Global Climate/Middle Atmosphere Model Part II: Model variability due to interactions between planetary waves, the mean circulation and gravity wave drag. *J. Atmos. Sci.*, **45**, 371–386.
- , ———, ———, and M. Prather, 1990: Climate change and the Middle Atmosphere. Part 1. The doubled CO<sub>2</sub> climate. *J. Atmos. Sci.*, **47**, 475–494.
- and A. Lacis, 1993: Climate change and the

- Middle Atmosphere. *Surveys in Geophysics*, **14**, 133–165.
- and N.K. Balachandran, 1995: Modeling the effects of solar variability and the QBO in the Troposphere/Stratosphere system. Part 2: The Troposphere. *J. Climate*, **8**, 2080–2095.
- , D. Shindell, P. Lonergan, P. and N.K. Balachandran, 1998: Climate change and the middle atmosphere. Part III: The Doubled CO<sub>2</sub> climate revisited. *J. Climate*, **11**, 876–894.
- , J. Lerner, and C. McLinden, 2001: Changes of tracer distributions in the doubled CO<sub>2</sub> climate. *J. Geophys. Res.* **106**, 28061–28079.
- Shindell, D., R. Miller, G. Schmidt, and L. Pandolfo, 1999a: Simulation of recent northern winter climate trends by greenhouse-gas forcing. *Nature*, **399**, 452–455.
- , D. Rind, N. Balachandran, J. Lean, and P. Lonergan, 1999b: Solar cycle variability, ozone and climate. *Science*, **284**, 305–308.
- Shindell, D.T., G.A. Schmidt, R.L. Miller, and D. Rind, 2001: Northern Hemisphere winter climate response to greenhouse gas, ozone, solar and volcanic forcing. *J. Geophys. Res.*, **106**, 7193–7211.
- Thompson, D.W. and J.M. Wallace, 2000: Annular modes in the extratropical circulation. Part I: Month-to month variability. *J. Climate*, **13**, 1000–1016.
- , ———, and G.C. Hegerl, 2000: Annular modes in the extratropical circulation. Part II: Trends. *J. Climate*, **13**, 1018–1036.
- Trenberth, K.E. and D.A. Paolino, 1980: The Northern Hemisphere sea level pressure dataset: Trends, errors and discontinuities. *Mon. Wea. Rev.* **108**, 855–872.
- van Loon, H. and K. Labitzke, 1988: Association between the 11-year solar cycle, the QBO and the atmosphere. Part II: Surface and 700 mb in the northern hemisphere winter. *J. Climate*, **1**, 905–920.
- Wiin-Nielsen, A., 2001: On the stability of atmospheric waves with low wave numbers. *Atmosfera*, **14**, 1–16.